Portable System for On-site Medical Spectral Imaging: Pre-clinical Development and Early Evaluation

Piotr Bartczak[1], Matti Iso-Mustajarvi[1], Hana Vrzakova[2], Roman Bednarik[2], Mikael Fraunberg[1], and Antti-Pekka Elomaa[1]

[1]Eastern Finland Center of Microsurgery, Kuopio University Hospital, Kuopio, Finland
Email: {piotr.bartczak,matti.iso-mustajarvi, mikael.fraunberg,antti-pekka.elomaa}@kuh.fi

[2]School of Computing, University of Eastern Finland, Joensuu, Finland
Email: {hanav,roman.bednarik}@uef.fi

***Abstract*—Imaging is an integral part of most operating room procedures and is used on a daily basis in the operating theater. Near real-time imaging during surgical procedures can significantly enhance the procedures by providing information about the anatomy and pathological conditions. So far, customizable spectral-imaging systems were only rarely investigated, developed and even less often installed in operational settings, especially microsurgery. In this paper we describe a design of portable imaging system for high throughput spectral characterization of ex vivo samples. The setup presented in this work was used for non-invasive collection of spectral signatures from a set of biological tissues.**

***Keywords*-Spectral imaging, surgery assistance, optical diagnostics for medicine, portable imaging system, medical optics instrumentation.**

I. Introduction

In surgical procedures concerning tumors, the physician aims to remove the tumor mass with a sufficient margin of normal tissue. Even under the high magnification, however, it is challenging to differentiate regions between the tumor and the healthy tissue, resulting in incomplete removal of the disease or in excision of negative margins [1, 2].

Spectral signatures of biological tissues are unique and especially in image guided procedures could significantly improve surgeon's decision making. Using near-real time contrast enhancement, spectral imaging can increases a likelihood of the complete tumor removal, and help to guide the surgery [3, 4].

One way how to support the intra-operative decision making is to analyze neurosurgery biopsies recorded during a surgery. In this case, a small sample of tumor candidates is extracted and sent to pathology laboratory for histological diagnosis [5, 6]. To properly detect the borders of a tumor, the procedure is usually repeated several times. As the pathological diagnosis is relatively inefficient and time consuming, the surgery gets delayed.

To improve and speed up this process, we propose and develop a *portable spectral system* to be used on-site or in the operating room. The system could significantly reduce the time of the first diagnosis and thus, decrease the total time of the surgery. Consequently, re-excision rate and lighten treatment related to expenses could be reduced.

Optical imaging techniques provide a novel non-invasive approach to characterize a composition of biological tissue. However, optical properties of medical features-of-interest are tightly connected to the type of observed tissue. Therefore, selection of an appropriate imaging system for medical analysis and procedure is rather challenging without prior understanding of the spectral properties of the particular tissue.

We developed and clinically tested a spectral imaging system based on Liquid Crystal Tunable Filter (LCTF), and acquired a set of images from ex vivo human tissue samples using our system. The spectral setup consists of an LCTF device, a monochrome camera and optical components. The measuring region for the system ranges from 400 to 720 nm of the spectra with 5 nm increment. The full resolution spectral image consists of 65 wavelength channels that are acquired in less than 16 seconds. The setup of portable spectral imaging system is illustrated in Figure 3.

In this work, we present an optical imaging system and evaluate its functionality in the visible region of the spectrum. Additionally, we apply our system to collect a spectral database of human tissues. Contrary to optical devices in the laboratory setting, our system is lightweight and portable, easily applicable at various stages at almost all clinical settings in the hospital. To our best knowledge, no such commercial medical imaging device exists, neither does a publicly available spectral database.

A. Spectral imaging in medical applications

Spectral imaging has recently received considerable attention in medical and clinical applications due to the efficiency, reliability, and design flexibility [3, 5]. Spectral imaging provides a noninvasive method to quantify spectral information from light reflected of the tissue. Images generated from

the spectral systems can be optically and computationally manipulated to make certain structures visible [7].

Prior research has investigated the notable enhancement in chromatic contrast and entropy analysis for illumination of tissues [8, 6]. Particularly in medical imaging, the spectral enhancements have been employed in lesion detection [8], retinal disease [9], and blood flow through tissue [10].

Image contrast enhancement, based on spectral information and optimized spectral distribution (SPD), in particular [9], has been previously studied under optimal and conventional illumination [11], however, such illumination is unoptimized and thus, unsuitable for contrast enhancement. Contrary to prior practice, we propose computed illumination optimized for diverse features and tissues as an alternative to the commonly employed broadband light since the computed illumination has potentials to simplify in vivo examinations through enhanced image quality [12, 13].

Recently, LCTF-based systems have received attention in various medical application [14, 15, 16]. Rapid non-mechanical filter adjustment makes LCTF best suited technology for clinical development, optical imaging and characterization of biological composition tissues [17, 18, 2].

B. Segmentation and analytic methods

In principle, spectral imaging provides rich spectral information instead of the typically employed RGB channels. Since the size of captured spectral cube is much larger, image acquisition, processing, computational analysis, and visualization of spectral data is adequately time demanding.

Various methods of spectral image processing have been developed for feature extraction [19], contrast enhancing [20], color discrepancy [21] and spectral cube compression [22]. Among these techniques Principal Component Analysis (PCA) has been particularly fruitful in reducing of the acquired spectral dataset [22]. PCA transforms the original high-dimensional correlated dataset into a substantially smaller datasets of uncorrelated features that represent the majority of the information stored in the original dataset. PCA has been also applied as a tool for extraction of interesting features from the spectral images [23]. The usage of PCA in spectral data analysis and segmentation has been studied in prior research [15, 21, 24].

Another commonly employed method for spectral image compression, optimal filter selection, and feature extraction is Non-Negative Tensor Factorization (NTF) [22, 23]. Optimal filters obtained from NTF have been employed to enhance the contrast between selected tissues without any need of post-processing [20, 9]. To reveal important spectral components in the sample, Independent Component Analysis (ICA), Multivariate Curve Resolution (MCR), wavelet compression, Learning Vector Quantization (LVQ), and Support Vector Machine (SVM) have been promising in the context of spectral imaging [25, 26, 27, 3].

Dataset complexity and repeated iterations needed for convergence to the correct solution, however, make the analysis of spectral images time-consuming. To simplify the computational demands, frequently used technique for an effective classification have been grounded on band ratio images [19].

Dividing an image of specific spectral component by the image of another one is able to provide unique information that are not revealed in single spectral image of the spectral cube in short time. Similarly, Normalized Difference Index (NDI), as a combination of reflectance and intensity, is a powerful method to enhance the differences in organs or tissues. Moreover, NDI might reveal the spectral differences in real-time [3].

II. Methods

A. Imaging system design and system description

The on-site imaging system was designed to perform reflectance spectral imaging in the visible range (400-720 nm). The system is based on a liquid-crystal tunable filter (VariSpec VIS-20, CRi, Inc.). The high-power, broadband halogen fiber optic illuminator (Thorlabs OSL2, Thorlabs, Inc.) was used as a primary light source. The single-output fiber bundle (Thorlabs OSL2FB, Thorlabs, Inc.) was employed for light guidance to the entrance port of the LCTF device. The light emerging from the fiber was collimated by the collimating package (Thorlabs OSL2COL, Thorlabs, Inc.), filtered, and focused into microscope ring illuminator (Thorlabs FRI61F50, Thorlabs, Inc.), dedicated for the OSL2 fiber light source.

The ring illuminator provides a bright, uniform, 360°, shadow-free illumination area. The illuminated area was captured by the monochrome CMOS camera (Thorlabs 3240CP-

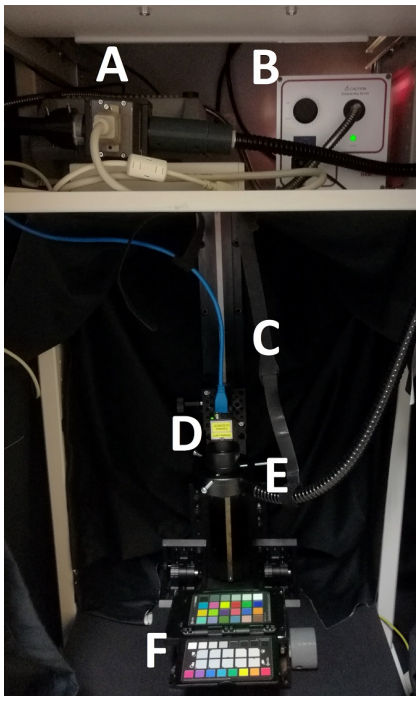

Fig. 1. Overview of the developed system for spectral imaging in the clinical environment. (A) LCTF device, (B) Broadband light source, (C) Manual linear translation stages, (D) Monochrome camera with objective, (E) Ring illuminator, (F) Linear stage for a specimen.

Requirements	Specification	Level
Setup and imaging time	Full operation of the equipment has to be obtained in short time. Complete imaging is limited to several minutes for ex vivo specimen and to several seconds for in vivo imaging.	Crucial
Portability	The size of the system has to allow deployment in surgical operating rooms. The equipment cannot take too much space in corridors or rooms.	Crucial
Accuracy and repeatability	Large similarity between measured and reference spectra has to be obtained. Repeated measurements under unchanged conditions show the same results.	Crucial
Operational feasibility	The design of equipment and imaging procedure have to be easy and intuitive. The systems has to always provide a robust and reliable output.	Crucial
Sterility	The system cannot produce any waste or toxic gases (e.g. ozone). It has to be free from live bacteria or other microorganisms. Sample container has to be easily replaceable.	Optional
Ergonomics	The design of medical equipment has to be focused on the needs of the end users: practitioners and specialists. The interaction between human and designed system has to guarantee its usability. Understanding human limitations in early stage of the development can reduce errors.	Crucial

TABLE I
REQUIREMENTS DERIVED FOR DESIGN AND IMPLEMENTATION OF A PORTABLE SPECTRAL IMAGING SYSTEM. A REQUIREMENT CAN EITHER BE CRITICAL (MUST-HAVE) OR OPTIONAL.

M, Thorlabs, Inc.) providing high resolution images (1280 x 1024 pixels). The c-mount lens (Tamron Co., Ltd) and manual linear translation stage were used for camera positioning and zooming. The synchronization of the LCTF device and the camera was implemented in custom C++ scripts and allowed for an automatic image sequence acquisition.

The system was completely embedded into a mobile electronics cart (Knurr EliMobile). Light trapping material was used inside for stray light suppression. Additionally, a light absorbing cloth was used to cover the mobile cart to prevent the ambient light pollution.

In collaboration with spectral imaging, medical, and clinical academics and professionals, we derived a set of requirements that a portable on-site medical spectral imaging system should optimally fulfill, see Table I. The imaging device fulfills all requirements and can be easily carried into a operating room or an endoscopy suite and then, set up within minutes using a laptop computer. The complete setup is presented in Figure 1.

B. Spectral calibration

We systematically evaluated spectral properties of the proposed system. The spectral sensitivity of described LCTF-based imaging system was determined by a combination of the spectral output of following: the primary light source, the transmittance of the LCTF and the ring illuminator, the sensitivity of the monochrome camera and the transmittance of the zoom lens. To simplify the calibration procedure, the LCTF-based spectral system was treated as a single unit in the calibration procedures.

Before each imaging trial, the following procedure was applied for system calibration. To obtain the original spectral response of the system and to correct influence of nonuniform illumination, a 99% diffuse Spectralon white reference sample (Spectralon, Labsphere, Inc.) was scanned across the tuning range of the LCTF (400 to 720 nm with 5 nm increments). While scanning, the optimal exposure time for each spectral band was calculated and used for further imaging.

Next, the dark images for the same spectral range were measured while keeping primary light source switched off. The dark images provided the information related to the internal noise of the camera.

Finally, a wavelength calibration procedure was established using illuminance spectrophotometer (Konica Minolta, CL-500A). The spectral power distribution (SPD) of light passing through the LCTF device and the ring illuminator was obtained (see Figure 2). The peak transmittance of each tunned filter was calculated and adapted. A thick black cloth used to completely block the outside ambient light was applied for every imaging and calibration step (see Figure 3).

The collected white and dark reference images were utilized for spectral reflectance calibration to normalize the intensity values of original spectral images. The reflectance was obtained from raw images using Formula 1:

$$I_R = \frac{I_{raw} - I_{dark}}{I_{white} - I_{dark}} \tag{1}$$

where I_R is the corrected relative reflectance image, I_{raw} is the original image without any corrections, I_{white} is the white reference image obtained from calibration procedure using Spectralon white reference, and I_{dark} is the dark image.

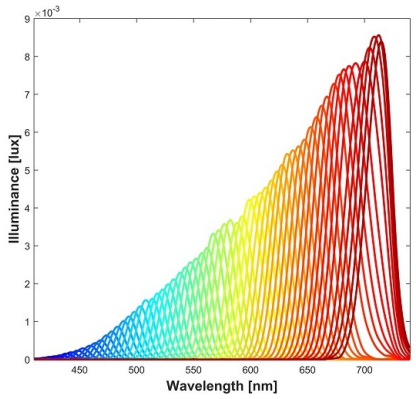

Fig. 2. Measured spectral power distribution of the light at the end of the ring illuminator. Intensity of each spectral bands depends strongly on a primary light source used together with LCTF device.

Fig. 3. The photograph of the spectral imaging system inside wet lab during specimen preparation. The small physical size allows for easy to move from place to place.

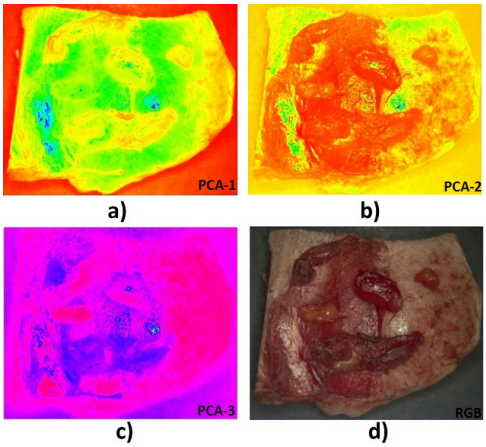

Fig. 5. Example of using PCA procedure as a band transformation method: (a) First inner product image, (b) Second inner product image, (c) Third inner product image, (d) Calculated RGB-image from full range spectral measurement of studied tissues.

C. Tissue handling and data acquisition

The imaging system capabilities were tested in several different ex vivo tissues. Trials were conducted in the wet lab at the Eastern Finland Center of Microsurgery in Kuopio University Hospital (see Figure 3) with respect to ethical permissions and the institutional approval. In this study, we used tissues from freshly frozen temporal bones. Images were taken immediately after defrost and preparation. Sample tissues were dissected and prepared by ENT (an ear, nose and throat) specialist. We managed to dissect and classify following tissues: bone, dura mater, muscle, fat, and carotid artery.

Tissues were placed on a dark non-fluorescent specimen tray and placed under the camera. The full imaging was consisted of successive grayscale frames acquired while tuning peak wavelength of the LCTF across its spectral range (400-720nm). To compensate the differences in system sensitivity, we varied the exposure times of the system camera. Identical exposure times settings were used for white and dark reference, needed for spectral reflectance as described before.

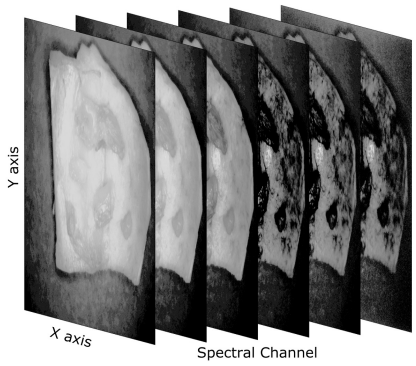

Fig. 4. Structure of a spectral image cube acquired by presented system with two dimensions (X,Y) of spatial information and one dimension (wavelength) of spectral information. Presented channels correspond to the images acquired by filters set at 712nm, 662nm, 613nm, 562nm, 514nm, 464nm, respectively (starting from the left).

Complete scanning across all filters took less than 16 seconds and resulted in 65 two-dimensional grayscale images that were employed to construct a three-dimensional spectral image cube (see Figure 4).

When the imaging was completed, the tissues were returned for processing and storage; the spectral images were immediately available for further evaluation. The advantage of the procedure is that the specimen never leaves the environment where it was procured, thus reduces time required for manipulation and regulatory concerns.

III. Results

Visualizations of multi-spectral images are available in real-time, however, spectral dimension reduction has to be applied first. For this purpose, we applied PCA based on eigen-decomposition. Figure 5 demonstrates first three inner product images and calculated RGB.

The first eigenvector is positive, holds the mean data of the spectral cube, and describes the majority of the variation inside the image. The second eigenvector produces the second largest variation of the image, third represents the third largest one, and so forth. Due to eigenvector independence and orthogonality, image inner products and their combinations are excellent candidates for feature extraction and tissue segmentation. Corresponding inner product images, used as an example of rapid tissue contrast enhancement, are shown in Figure 5.

To demonstrate the functionality of the system, we acquired a collection of spectral signatures from the available tissues with corresponding spectral reflectance from 400 to 720 nm in 5 nm increments and are plotted in Figure 6. Spectral signatures of all captured biological tissues were unique and the biggest differences could be noticed especially between areas of a bone and dura. Real-time contrast enhancement

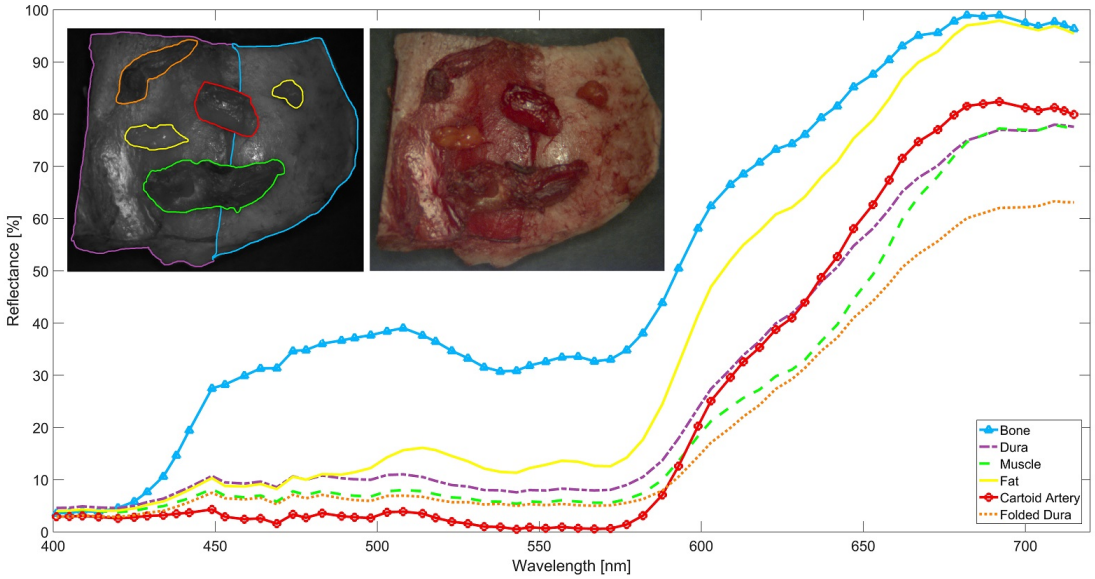

Fig. 6. Gray scale image for spectral band at 555nm used for annotations of measured ex vivo tissues made by ENT specialist (top left) and corresponding RGB image of the specimen (top right). Spectral reflectance curve of following tissues: bone, dura, muscle, fat, carotid artery, and folded dura. Reflectance was obtained from manually selected area of the image within annotated borders. Color of each curve corresponds to the same color used for area annotation.

between these two tissues was obtained by the peak wavelength selection using developed software. The best results were obtained and instantly displayed on the screen for the LCTF settings between 450-570 nm, (see Figure 4).

IV. Discussion

A portable spectral imaging system was tested in clinical environment. During pre-clinical testing, spectral signatures of several different ex vivo tissues were acquired. Spectral signatures are presented and their difference in spectral properties in visible range are shown. The proposed portable imaging system presents an excellent instrument for obtaining reflectance collection resulting in a spectral database. The system allows for processing of voluminous spectral data in real-time and could be a significant breakthrough in designing new medical systems e.g., tunable illumination, optical filters, and decision-aid systems. Current medical applications related to spectral imaging are practically infeasible because of the slow processing times. Spectral signatures collected using proposed system could help to find and evaluate appropriate intensity and reflectance channels used for NDI, resulting in a lower number of spectral bands being captured and reduced computation time. Finally, spectrally enhanced visualizations of biological tissues could offer valuable information for physicians and surgeons in a real-time.

Additionally, spectral information provided by our proposed system allows non-invasive examination and classification of tissues. First and second inner product images in the presented example could be used to simplify the estimation of the edge between bone and dura tissues or to estimate the area of each tissue.

As illustrated in Figure 5 (a) and (b), green color in the image of the first inner product corresponds to the area classified as the bone tissue. It is noticeable that thinner layer of dura is represented by the combination of green and yellow color. This is caused by a smaller portion of light being absorbed by dura tissue in the region and consequently, by higher influence of optical properties reflected from the bone tissue. The tissue characterization could be fruitful in future applications to estimate the thickness of dura's layer. The second inner product localized well the area with the dura tissue. Corresponding figure reveals well the enhanced contrast between bone and the remaining parts of dura (presented by the red color) after the attempt of its complete removal by the specialist. This example demonstrates how the presented portable imaging system could be employed as a visual supporting tool during examination and diagnosis.

We propose the LCTF based spectral imaging system for on-site database collection. The setup is applicable in various applications: neurosurgical procedures including demanding resections such as tumour, epilepsy or spinal surgery, and ear-nose-throat operations such as cholesteatoma.

V. Future Research

The reported tissue separation was based on visual evaluations of an expert neurosurgeon and presents preliminary tests to show results delivered by our developed imaging system. In future work, we will extend the systematic evaluation with further studies with pathological reports, including quantitative information and evaluation with respect to tissue classification.

The presented tissue database will be gradually extended for examining the cutoffs due to unique tissue characteristics and will include fresh samples of both pathological and healthy samples. The capability of imaging system will be extended to the illumination range including ultraviolet and near-infrared wavelengths, as an addition to adjustable light

source. Ultimately, we aim for adjustable camera capable of auto-fluorescent enhancement.

VI. Acknowledgments

We want to acknowledge help of the University of Eastern Finland, Computational Spectral Imaging Research Laboratory, especially Joni Hyttinen, and Pauli Fält, for participating in software development used for the setup control. The work was supported by Academy of Finland, Grant no. 305199.

References

[1] D. A. Orringer, A. Golby, and F. Jolesz, "Neuronavigation in the surgical management of brain tumors: current and future trends," *Expert review of medical devices*, vol. 9, no. 5, pp. 491–500, 2012.

[2] S. C. Gebhart, D. L. Stokes, T. Vo-Dinh, and A. Mahadevan-Jansen, "Instrumentation considerations in spectral imaging for tissue demarcation: comparing three methods of spectral resolution," in *Spectral Imaging: Instrumentation, Applications, and Analysis III*, vol. 5694. International Society for Optics and Photonics, 2005, pp. 41–53.

[3] H. Akbari and Y. Kosugi, "Hyperspectral imaging: A new modality in surgery," in *Recent advances in biomedical engineering*. InTech, 2009.

[4] S. C. Gebhart and A. Mahadevan-Jansen, "Brain tumor demarcation with liquid-crystal tunable filter spectral imaging," in *Advanced Biomedical and Clinical Diagnostic Systems IV*, vol. 6080. International Society for Optics and Photonics, 2006, p. 60800I.

[5] R. Levenson, J. Beechem, and G. McNamara, "Spectral imaging in preclinical research and clinical pathology," *Analytical Cellular Pathology*, vol. 35, no. 5, 6, pp. 339–361, 2012.

[6] S. A. Toms, W.-C. Lin, R. J. Weil, M. D. Johnson, E. D. Jansen, and A. Mahadevan-Jansen, "Intraoperative optical spectroscopy identifies infiltrating glioma margins with high sensitivity," *Operative Neurosurgery*, vol. 57, no. suppl_4, pp. ONS–382, 2005.

[7] S. V. Panasyuk, S. Yang, D. V. Faller, D. Ngo, R. A. Lew, J. E. Freeman, and A. E. Rogers, "Medical hyperspectral imaging to facilitate residual tumor identification during surgery," *Cancer biology & therapy*, vol. 6, no. 3, pp. 439–446, 2007.

[8] D. Nouri, Y. Lucas, and S. Treuillet, "Infrared hyperspectral imaging for enhanced tissue visualization and discrimination during surgical operation," in *Image Processing (ICIP), 2014 IEEE International Conference on*. IEEE, 2014, pp. 5137–5141.

[9] P. Bartczak, P. Fält, N. Penttinen, P. Ylitepsa, L. Laaksonen, L. Lensu, M. Hauta-Kasari, and H. Uusitalo, "Spectrally optimal illuminations for diabetic retinopathy detection in retinal imaging," *Optical Review*, vol. 24, no. 2, pp. 105–116, 2017.

[10] J. H. Klaessens, R. De Roode, R. M. Verdaasdonk, and H. J. Noordmans, "Hyperspectral imaging system for imaging o 2 hb and hhb concentration changes in tissue for various clinical applications," in *Advanced Biomedical and Clinical Diagnostic Systems IX*, vol. 7890. International Society for Optics and Photonics, 2011, p. 78900R.

[11] P. Bartczak, P. Fält, and M. Hauta-Kasari, "Applicability of led-based light sources for diabetic retinopathy detection in retinal imaging," in *Computer-Based Medical Systems (CBMS), 2016 IEEE 29th International Symposium on*. IEEE, 2016, pp. 355–360.

[12] P. Liu, H. Wang, Y. Zhang, J. Shen, R. Wu, Z. Zheng, H. Li, and X. Liu, "Investigation of self-adaptive led surgical lighting based on entropy contrast enhancing method," *Optics Communications*, vol. 319, pp. 133–140, 2014.

[13] P. Bartczak, A. Gebejes, P. Fält, and M. Hauta-Kasari, "An led-based tunable illumination for diverse medical applications," in *Computer-Based Medical Systems (CBMS), 2016 IEEE 29th International Symposium on*. IEEE, 2016, pp. 292–293.

[14] Y. Hirohara, Y. OKawa, T. Mihashi, T. Yamaguchi, N. Nakazawa, Y. Tsuruga, H. Aoki, N. Maeda, I. Uchida, and T. Fujikado, "Validity of retinal oxygen saturation analysis: Hyperspectral imaging in visible wavelength with fundus camera and liquid crystal wavelength tunable filter," *Optical review*, vol. 14, no. 3, p. 151, 2007.

[15] J. Antikainen, M. von Und Zu Fraunberg, J. Orava, J. E. Jaaskelainen, and M. Hauta-Kasari, "Spectral imaging of neurosurgical target tissues through operation microscope," *Optical review*, vol. 18, no. 6, pp. 458–461, 2011.

[16] C. Hoyt, "Liquid crystal tunable filters clear the way for imaging multiprobe fluorescence," *Biophotonics International*, vol. 4, pp. 49–51, 1996.

[17] S. C. Gebhart, R. C. Thompson, and A. Mahadevan-Jansen, "Liquid-crystal tunable filter spectral imaging for brain tumor demarcation," *Applied optics*, vol. 46, no. 10, pp. 1896–1910, 2007.

[18] J.-H. Lee and C.-H. Won, "Characterization of lung tissues using liquid-crystal tunable filter and hyperspectral imaging system," in *Engineering in Medicine and Biology Society, 2009. EMBC 2009. Annual International Conference of the IEEE*. IEEE, 2009, pp. 1416–1419.

[19] D. P. Ariana, R. Lu, and D. E. Guyer, "Near-infrared hyperspectral reflectance imaging for detection of bruises on pickling cucumbers," *Computers and electronics in agriculture*, vol. 53, no. 1, pp. 60–70, 2006.

[20] K. Nishino, M. Nakamura, M. Matsumoto, O. Tanno, and S. Nakauchi, "Imaging of cosmetics foundation distribution by a spectral difference enhancement filter," in *Conference on Colour in Graphics, Imaging, and Vision*, vol. 2010, no. 1. Society for Imaging Science and Technology, 2010, pp. 275–281.

[21] G. Polder, G. W. van der Heijden, and I. T. Young, "Tomato sorting using independent component analysis on spectral images," *Real-time imaging*, vol. 9, no. 4, pp. 253–259, 2003.

[22] J. Lehtonen, M. Hauta-Kasari, J. Parkkinen, and T. Jaaskelainen, "Image format for spectral image browsing," *Journal of Imaging Science and Technology*, vol. 50, no. 6, pp. 572–582, 2006.

[23] A. Andriyashin, J. Parkkinen, and T. Jaaskelainen, "Illuminant dependence of pca, nmf and ntf in spectral color imaging," in *Pattern Recognition, 2008. ICPR 2008. 19th International Conference on*. IEEE, 2008, pp. 1–4.

[24] J. Y. Qu, H. Chang, and S. Xiong, "Fluorescence spectral imaging for characterization of tissue based on multivariate statistical analysis," *JOSA A*, vol. 19, no. 9, pp. 1823–1831, 2002.

[25] B. Du, N. Wang, L. Zhang, and D. Tao, "Hyperspectral medical images unmixing for cancer screening based on rotational independent component analysis," in *International Conference on Intelligent Science and Big Data Engineering*. Springer, 2013, pp. 336–343.

[26] S. Sindhumol, A. Kumar, and K. Balakrishnan, "Spectral clustering independent component analysis for tissue classification from brain mri," *Biomedical Signal Processing and Control*, vol. 8, no. 6, pp. 667–674, 2013.

[27] H. Xu and B. W. Rice, "In-vivo fluorescence imaging with a multivariate curve resolution spectral unmixing technique," *Journal of biomedical optics*, vol. 14, no. 6, p. 064011, 2009.